

PMD compensation in fiber-optic communication systems with direct detection using LDPC-coded OFDM

Ivan B. Djordjevic

University of Arizona, Department of Electrical and Computer Engineering, Tucson, AZ 85721, USA
ivan@ece.arizona.edu

Abstract: The possibility of polarization-mode dispersion (PMD) compensation in fiber-optic communication systems with direct detection using a simple channel estimation technique and low-density parity-check (LDPC)-coded orthogonal frequency division multiplexing (OFDM) is demonstrated. It is shown that even for differential group delay (DGD) of $4/BW$ (BW is the OFDM signal bandwidth), the degradation due to the first-order PMD can be completely compensated for. Two classes of LDPC codes designed based on two different combinatorial objects (difference systems and product of combinatorial designs) suitable for use in PMD compensation are introduced.

©2007 Optical Society of America

OCIS codes: (060.4510) Optical communications; (999.9999) Polarization mode dispersion (PMD); (060.4080) Modulation; (060.4230) Multiplexing; (999.9999) Orthogonal frequency division multiplexing; (999.9999) Low-density parity-check (LDPC) codes

References and Links

1. H. F. Haunstein, W. Sauer-Greff, A. Dittrich, K. Sticht, and R. Urbansky, "Principles for electronic equalization of polarization-mode dispersion," *J. Lightwave Technol.* **22**, 1169-1182 (2004).
2. M. Jäger, T. Rankl, J. Spiedel, H. Bulow, and F. Buchali, "Performance of turbo equalizers for optical PMD channels," *J. Lightwave Technol.* **24**, 1226-1236 (2006).
3. I. B. Djordjevic, and B. Vasic, "Nonlinear BCJR equalizer for suppression of intrachannel nonlinearities in 40 Gb/s optical communications systems," *Opt. Express* **14**, 4625-4635 (2006).
4. L. R. Bahl, J. Cocke, F. Jelinek, and J. Raviv, "Optimal decoding of linear codes for minimizing symbol error rate," *IEEE Trans. Inf. Theory* **IT-20**, 284-287 (1974).
5. C. Douillard, M. Jézéquel, C. Berrou, A. Picart, P. Didier, and A. Glavieux, "Iterative correction of intersymbol interference: turbo equalization," *Eur. Trans. Telecommun.* **6**, 507-511 (1995).
6. I. B. Djordjevic, H. G. Batshon, M. Cvijetic, L. Xu, and T. Wang, "PMD compensation by LDPC coding based turbo equalization," *IEEE Photon. Technol. Lett.*, submitted for publication.
7. R. van Nee, and R. Prasad, *OFDM Wireless Multimedia Communications* (Artech House, Boston 2000).
8. A. J. Lowery, L. Du, and J. Armstrong, "Orthogonal frequency division multiplexing for adaptive dispersion compensation in long haul WDM systems," in *Proc. OFC Postdeadline Papers*, Paper no. PDP39, 2006.
9. I. B. Djordjevic and B. Vasic, "Orthogonal frequency-division multiplexing for high-speed optical transmission," *Opt. Express* **14**, 3767-3775 (2006).
10. I. B. Djordjevic, and B. Vasic, "100 Gb/s transmission using orthogonal frequency-division multiplexing," *IEEE Photon. Technol. Lett.* **18**, 1576-1578 (2006).
11. W. Shieh, W. Chen and R.S. Tucker, "Polarization mode dispersion mitigation in coherent optical orthogonal frequency division multiplexed systems," *Electron. Lett.* **42**, 996-997 (2006).
12. W. Shieh, and C. Athaudage, "Coherent optical frequency division multiplexing," *Electron. Lett.* **42**, 587-589 (2006).
13. W. Shieh, "PMD-supported coherent optical OFDM systems," *IEEE Photonics Technol. Lett.* **19**, 134-136 (2006).
14. A. J. Lowery, and J. Armstrong, "10 Gb/s multimode fiber link using power-efficient orthogonal-frequency-division multiplexing," *Opt. Express* **13**, 10003-10009 (2005).
15. M. Cvijetic, *Coherent and Nonlinear Lightwave Communications* (Artech House, Boston 1996).
16. A. Garcia Armada and M. Calvo, "Phase noise and sub-carrier effects on the performance of an OFDM communication system," *IEEE Commun. Lett.* **2**, 11-13 (1998).
17. I. B. Djordjevic, S. Sankaranarayanan, S. K. Chilappagari, and B. Vasic, "Low-density parity-check codes for 40 Gb/s optical transmission systems," *IEEE J. Sel. Top. Quantum Electron.* **12**, 555-562 (2006).
18. I. Anderson, *Combinatorial Designs and Tournaments* (Oxford University Press, 1997).

19. D. Raghavarao, *Constructions and Combinatorial Problems in Design of Experiments* (Dover Publications, New York, 1988).
20. C.-C. Lin, K.-L. Lin, H.-Ch. Chang, and C.-Y. Lee, "A 3.33Gb/s (1200,720) low-density parity check code decoder," in Proc. ESSCIRC 2005, 211-214 (2005), Grenoble, France.
21. M. Morelli and U. Mengali, "A comparison of pilot-aided channel estimation methods for OFDM systems," *IEEE Trans. Signal Process.* **49**, 3065-3073 (2001).
22. M. N. Vartak, "On application of Kronecker product of matrices to statistical designs," *Ann. Math. Stat.* **26**, 420-438 (1955).
23. O. Milenkovic, I. B. Djordjevic, and B. Vasic, "Block-circulant low-density parity-check codes for optical communication systems," *IEEE J. Sel. Top. Quantum Electron.* **10**, 294-299 (2004).
24. B. Vasic, I. B. Djordjevic, and R. Kostuk, "Low-density parity check codes and iterative decoding for long haul optical communication systems," *J. Lightwave Technol.* **21**, 438-446 (2003).
25. D. J. C. MacKay, "Encyclopedia of sparse graph codes," available at <http://www.inference.phy.cam.ac.uk/mackay/codes/data.html>

1. Introduction

The performance of fiber-optics communication systems operating at high-speed are degraded significantly due to several transmission impairments including intrachannel and interchannel fiber nonlinearities, Gordon-Mollenauer effect and polarization-mode dispersion (PMD) [1-3]. The PMD is quite challenging impairment to compensate due to its time variant and stochastic nature. Recently, several PMD electrical compensators have been proposed including Viterbi [1], Bahl-Cocke-Jelinek-Raviv (BCJR) [2-4], and turbo equalizers [5]. In our recent submission [6] we have shown that low-density parity-check (LDPC)-coded turbo equalizer is able successfully to tackle the differential group delay (DGD) up to two bit-periods for reasonable trellis complexity of the BCJR equalizer. However, for DGDs above two-bit periods the complexity of BCJR equalizer is prohibitively high for high-speed implementation, and some alternative approaches are to be found.

In this paper we will show that LDPC-coded orthogonal frequency division multiplexing (OFDM), supplemented with appropriate channel estimation is an excellent alternative to LDPC-coded turbo equalization. OFDM is a special case of multi-carrier transmission in which a single information-bearing stream is transmitted over many lower rate sub-channels, and has already been used or proposed for a variety of applications [7-10], including digital audio broadcasting, high-definition television (HDTV) broadcasting, high bit-rate digital subscriber line (DSL), IEEE 802.11 [7], radio-over-fiber-based links, free-space optical communications, long-haul optical communications systems [8-13], multimode fiber links [14], and 100-Gb/s Ethernet [10]. Due to orthogonality among sub-carriers in OFDM, partial overlap of neighboring frequency slots is allowed, thereby improving spectral efficiency as compared with a conventional multi-carrier system. Also, by using a sufficiently large number of sub-carriers and cyclic extension, the intersymbol interference (ISI) due to PMD can be reduced. To further reduce the distortion due to PMD we propose the use of a particular channel estimation technique, based on a short training sequence. For the first-order PMD compensation the training sequence is to be sent only once, before the start of a transmission. The proposed PMD compensation scheme is combined with advanced forward error correction (FEC) based on structured LDPC codes [17]. Two classes of structured high rate LDPC codes based on two different combinatorial objects, suitable for high-speed implementation are proposed. The first class is based on so called *difference systems* [18,19], and the second class is based on a concept of *product of combinatorial designs*, new concept introduced in Section 3. Because the state-of-the art fiber-optics communication systems employ the intensity modulation with direct detection (IM/DD), we consider the problem of PMD compensation in fiber-optics communications with direct detection only. The coherent optical OFDM requires the use of an additional local laser, and a polarization tracking receiver or polarization diversity increasing therefore the receiver complexity, and the implementation cost. Moreover, such a solution is sensitive to the laser phase noise because two laser sources (transmitting and receiving) are to be used.

The paper is organized as follows. In Section 2 we introduce the concept of PMD compensation by LDPC-coded OFDM. In Section 3 we describe two classes of LDPC codes

based on two different combinatorial objects, difference systems and a product of combinatorial designs. In Section 4 the numerical results are reported, and some important conclusions are given in Section 5.

2. PMD compensation by LDPC-coded OFDM

The transmitter and receiver configurations are shown in Fig. 1(a) and 1(b), respectively; while the OFDM symbol after cyclic extension is shown in Fig. 1(c). An information-bearing stream at 10 Gb/s is demultiplexed into four 2.5-Gb/s streams, which are further encoded using identical LDPC codes. This step is determined by currently existing LDPC chips [20]. The outputs of LDPC encoders are demultiplexed and parsed into groups of b_s bits corresponding to the OFDM symbol.

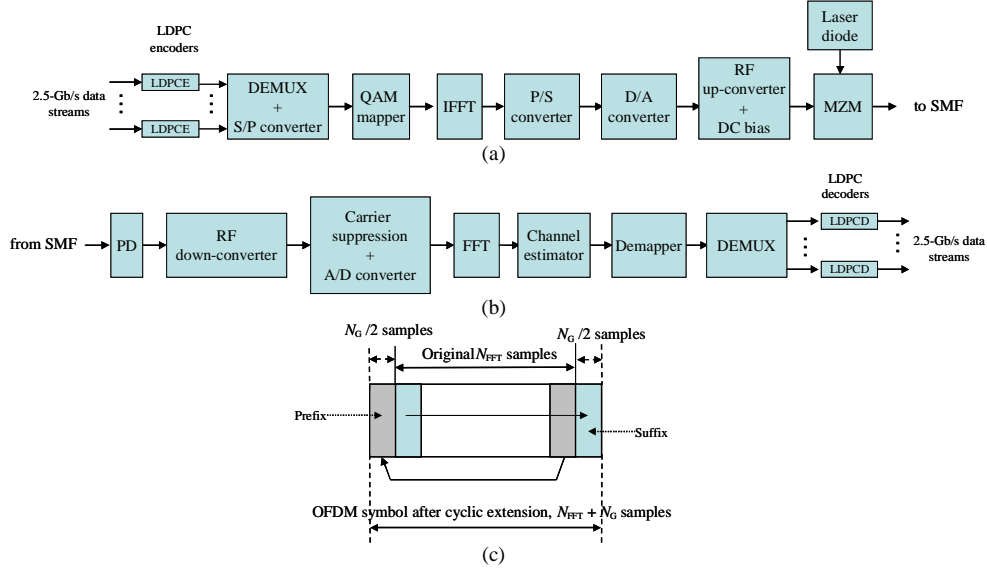


Fig. 1. Transmitter configuration (a), receiver configuration (b), and OFDM symbol after cyclic extension (c). LDPCE-LDPC encoder, LDPCD-LDPC decoder, S/P-serial-to-parallel converter, MZM-Mach-Zehnder modulator.

The b_s bits in each OFDM symbol are subdivided into K sub-channels with i^{th} sub-carrier carrying b_i bits, $b_s = \sum b_i$. The b_i bits from the i^{th} sub-channel are mapped into a complex-valued signal from a 2^{b_i} -point signal constellation such as QAM, which is considered in this paper, using Gray mapping. For example, $b_i=2$ for QPSK and $b_i=4$ for 16-QAM. The complex-valued signal points from sub-channels are considered to be the values of the discrete Fourier transform (DFT) of a multi-carrier OFDM signal. By selecting the number of sub-channels K , sufficiently large, the OFDM symbol interval can be made significantly larger than the dispersed pulse-width of an equivalent single-carrier system, resulting in significantly reduced ISI due to PMD. Following the description and notation given in Ref. [7], the OFDM signal in RF domain (after a D/A conversion and RF up-conversion) can be written as

$$s_{\text{OFDM}}(t) = \text{Re} \left\{ \sum_{k=-\infty}^{\infty} w(t-kT) \sum_{i=-(N_{\text{FFT}}/2)}^{(N_{\text{FFT}}/2)-1} X_{i,k} \cdot e^{j2\pi \frac{i}{T_{\text{FFT}}}(t-kT)} e^{j2\pi f_{\text{RF}} t} \right\} \quad (1)$$

$$kT - \left(\frac{T_G}{2} \right) - T_{\text{win}} \leq t \leq kT + T_{\text{FFT}} + \left(\frac{T_G}{2} \right) + T_{\text{win}}$$

where $X_{i,k}$ is the i -th subcarrier QAM symbol of the k -th OFDM symbol, T is the OFDM symbol duration, T_{FFT} is the FFT part duration, T_G is the guard interval duration (the duration

of cyclic extension), T_{win} is the length of the windowing interval, $w(t)$ is the window function, and f_{RF} is the RF carrier frequency. The OFDM symbol, shown in Fig. 1(c), is generated as follows: $N_{\text{QAM}}(=K)$ input QAM symbols are zero-padded to obtain N_{FFT} input samples for IFFT, the N_{G} samples are inserted to create the guard interval, and the OFDM symbol is multiplied by the window function. The purpose of cyclic extension is to preserve the orthogonality among sub-carriers even when the neighboring OFDM symbols partially overlap due to PMD, and the purpose of the windowing is to reduce the out-of-band spectrum. The cyclic extension, illustrated in Fig. 1(c), is done by repeating the last $N_{\text{G}}/2$ samples of the effective OFDM symbol part (N_{FFT} samples) as the prefix, and repeating the first $N_{\text{G}}/2$ samples as the suffix.

The OFDM signal in RF domain can be converted to optical domain using one of two possible options: (i) the OFDM signal can directly modulate the distributed feedback laser (DFB) laser, and (ii) the OFDM signal can be used as RF input of the MZM. In this paper we consider only the second option because the first option is sensitive to the frequency chirp of the light source. The *DC bias component* must be inserted (in RF domain) to enable recovering the QAM symbols incoherently. Because bipolar signals cannot be transmitted over an IM/DD link, it is assumed that the bias component is sufficiently large so that when added to the OFDM signal the resulting sum is non-negative. We refer to this scheme as biased-OFDM (B-OFDM). The main disadvantage of B-OFDM scheme is the poor power efficiency. To improve the power efficiency we can use the single-side band (SSB) transmission, and employ the clipping of the OFDM signal after bias addition. We refer to this scheme as clipped-OFDM (C-OFDM). Unfortunately, the clipping introduces the distortion of OFDM signal. To avoid distortion due to clipping we propose to transmit the information signal by modulating the electrical field (instead of intensity modulation) using an MZM so that negative part of OFDM signal can be transmitted towards the photodetector. Distortion introduced by the photodetector, caused by squaring, can be successfully eliminated by proper filtering [8-10]. The bias is varied to find the optimum one for fixed optical launched power. It was found that the optimum case is one in which ~50% of the total electrical signal energy is allocated for transmission of a carrier. We refer to this scheme as unclipped-OFDM (U-OFDM).

The receiver commonly employs the trans-impedance amplifier (TA) design, because it is a good compromise between noise and bandwidth. The PIN photodiode output current can be written as

$$i(t) = R \left\{ \left| \sqrt{k} \left(s_{\text{OFDM}}(t) + b \right) * h_V(t) \right|^2 + \left| \sqrt{1-k} \left(s_{\text{OFDM}}(t) + b \right) * h_H(t) \right|^2 \right\}, \quad (2)$$

where $s_{\text{OFDM}}(t)$ denotes the transmitted OFDM signal, b is the DC bias component, R denotes the photodiode responsivity, and k denotes the power-splitting ratio between two principal states of polarizations (PSPs) ($k=1/2$ corresponds to the worst-case scenario). For the first order PMD, the optical channel responses $h_H(t)$ and $h_V(t)$ corresponding to the horizontal and vertical PSPs are given respectively as [2] $h_H(t) = \delta(t + \Delta\tau/2)$ and $h_V(t) = \delta(t - \Delta\tau/2)$, where $\Delta\tau$ is the DGD of two PSPs. (The *-operator is the convolution operator.) The similar model has also been used in [2] for DGDs up to two bit-periods. The photodiode output signal, after appropriate filtering to remove the squared and DC terms, in the presence of the first order PMD is proportional to

$$i(t) \sim 2Rb \left[k \cdot s_{\text{OFDM}}(t - \Delta\tau/2) + (1-k) \cdot s_{\text{OFDM}}(t + \Delta\tau/2) \right], \quad (3)$$

and is very similar to a two-ray multipath wireless model [7], suggesting that similar channel estimation techniques can be employed. Notice that the power splitting ratio $k \in [0,1]$, so that for $k=0$ only the second term is present while for $k=1$ only the first term is present. Nevertheless, the delayed version of OFDM signal is present in both cases and transmitted signal can be successfully demodulated. In the presence of strong higher order PMD the polarization would be widely dispersed across the Poincare sphere as shown in Reg. [13]. The single-carrier system would be severely affected by strong PMD. However, the OFDM symbol detection is based on sub-carrier basis, and PMD is much less important at sub-carrier

level (see [13] for more details). To deal with higher order PMD effects, the OFDM symbols are to be organized in packets with the first packet and several pilots in every OFDM symbols being used to estimate channel coefficients, in a fashion similar to that presented in chapter 5 of reference [7].

The signal after RF down-conversion and carrier suppression can be written as

$$r(t) = \left[i(t) k_{RF} \cos(\omega_{RF} t) \right] * h_e(\tau) + n(t), \quad (4)$$

where $h_e(t)$ is the impulse response of the low-pass filter, $n(t)$ is electronic noise in the receiver (mostly due to TA thermal noise), commonly modeled as a Gaussian process, and k_{RF} denotes the RF down-conversion factor. Finally, after the A/D conversion and cyclic extension removal, the transmitted signal is demodulated by FFT algorithm. Following the derivation similar to that outlined in Ref. [7] (see also [11,12]), it can be shown that the received QAM symbol of i -th subcarrier of the k -th OFDM symbol is related to transmitted QAM symbol $X_{i,k}$ by

$$Y_{i,k} = h_i e^{j\theta_k} X_{i,k} + n_{i,k}, \quad (5)$$

where h_i is channel distortion introduced by PMD (and chromatic dispersion), and θ_k is the phase shift of k -th OFDM symbol due to chromatic dispersion and self-phase modulation (SPM). Notice that in the absence of chromatic dispersion and SPM, θ_k is actually equal to zero. However, the symbol phase noise due to SPM, and RF down-converter will be present. This kind of noise can successfully be tackled by pilot-aided channel estimation [21] (see also [9,10]). To determine the first-order PMD distortion coefficients h_i it is not necessary to transmit the pilot-tones, it is enough just to pre-transmit the short training OFDM sequence. In a decision-directed mode the transmitted QAM symbols are estimated by

$$\hat{X}_{i,k} = \left(h_i^* / |h_i|^2 \right) e^{-j\theta_k} Y_{i,k}. \quad (6)$$

To illustrate the validity of this approach in suppression of the first order PMD we performed a simulation, for OFDM system parameters given in Section 4, by employing 16-QAM-OFDM SSB transmission in the absence of noise. The signal constellation diagrams before, and after channel estimation for DGD of $4/BW$ (BW -the OFDM signal bandwidth) are given in Fig. 2(a) and Fig. 2(b), respectively. Obviously, the PMD distortion can be significantly reduced by using a simple training sequence. The simulation is performed for power-splitting ratio $k=1/2$, which corresponds to the worst case scenario. The corresponding LDPC-coded turbo equalization scheme we proposed in [6], requires the channel trellis with too many states to be of practical importance for this amount of DGD.

Notice that OFDM alone has already been recently considered for *coherent* optical communication systems [11]. However, as already mentioned in Introduction (see also [15]), such a solution requires the use of an additional local laser and either a polarization tracking receiver or polarization diversity [11], increasing therefore the receiver complexity. Also the state-of-the art optical communication systems already installed are essentially IM/DD systems, suggesting that PMD compensation technique proposed in this paper is timely, and much less expensive to implement. The significant advantage of using optical OFDM systems with direct detection is insensitivity to the laser phase noise. Because both polarization components are equally affected by the laser phase noise, to simplify explanation let us observe the case in the absence of PMD. Transmitted electrical field is proportional to

$$E(t) \sim e^{j[\omega_{DFB}t + \phi_{PN}(t)]} [s_{OFDM}(t) + b], \quad (7)$$

where ω_{DFB} is optical carrier frequency, while with $\phi_{PN}(t)$ we denoted the laser phase noise (PN) process. (s_{OFDM} and b are introduced earlier, and the RF carrier frequency f_{RF} is already incorporated in s_{OFDM} , see the Eq. (1).) The photodiode current is proportional to

$$i(t) \sim |E(t)|^2 \sim \left| e^{j[\omega_{DFB}t + \phi_{PN}(t)]} [s_{OFDM}(t) + b] \right|^2 = \left| e^{j[\omega_{DFB}t + \phi_{PN}(t)]} \right|^2 |s_{OFDM}(t) + b|^2 = |s_{OFDM}(t) + b|^2, \quad (8)$$

and it is completely insensitive to the laser phase noise. In coherent OFDM, the situation is quite different. Following the derivation similar to that given in Ref. [15], it can be shown that the balanced detector output is proportional to

$$v_{\text{balanced}}(t) \sim e^{j[(\omega_{\text{DFB1}} - \omega_{\text{DFB2}})t + \phi_{\text{PN1}}(t) - \phi_{\text{PN2}}(t)]} s_{\text{OFDM}}(t), \quad (9)$$

where ω_{DFB1} and ω_{DFB2} are the optical carrier frequencies of transmitting and receiving laser, respectively; while with $\phi_{\text{PN1}}(t)$ and $\phi_{\text{PN2}}(t)$ we denoted the laser phase noise processes of transmitting and receiving laser, respectively. (Notice that the biasing is not needed in coherent OFDM ($b=0$).) It is well known that the laser phase noise process can be modeled as Wiener-Lévy process [15] that is a zero-mean Gaussian process with variance $2\pi\Delta\nu|t|$, where $\Delta\nu$ is the laser linewidth. The resulting process $\phi_{\text{PN1}}(t) - \phi_{\text{PN2}}(t)$ is a zero-mean Gaussian with variance $2\pi(\Delta\nu_1 + \Delta\nu_2)|t|$, where with $\Delta\nu_1$ and $\Delta\nu_2$ we denoted the laser linewidths of transmitting and receiving laser, respectively.

Therefore, in OFDM systems with direct detection the laser phase noise is not important effect in performance degradation, while in coherent OFDM systems could introduce severe performance degradation for laser linewidths above 1 MHz. To compensate for the common phase error [16] due to laser phase noise in coherent OFDM systems, someone may want to use the pilot-aided channel estimation [21] (see also [9,10]). Moreover, if the phase variations due to laser phase noise are comparable or higher than OFDM period, the inter-carrier interference is becoming important and the laser phase noise cannot be completely eliminated by pilot-aided channel estimation. For more details on this problem an interested reader is referred to Ref. [16]. From reasons above we restricted our attention to the optical OFDM systems with direct detection.

Given this description of uncoded optical OFDM system with direct detection, we turn our attention to the design of LDPC codes suitable for PMD-compensation in Section 3, while numerical results for both uncoded and coded case are reported in Section 4.

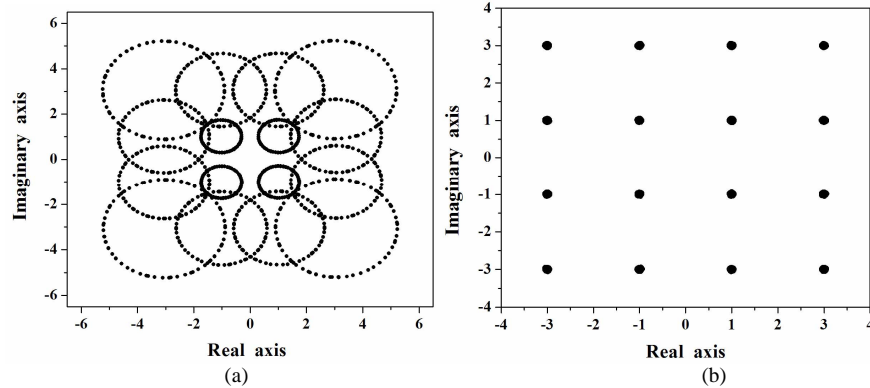


Fig. 2. Constellation diagrams before (a), and after (b) channel estimation for DGD equal to $4/BW$ (BW -the OFDM signal bandwidth), and $k=1/2$ in the absence of noise.

3. Design of high-rate LDPC codes

In this section we present two classes of LDPC codes of high-code rate, based on two different combinatorial objects: (i) difference systems [18, 19], and (ii) a product of combinatorial designs.

Definition 1. The sets S_1, \dots, S_t of size k are said to form a (v, k, λ) difference system (DS) over an additive abelian group V of order v , if the differences arising from S_i gives each nonzero element of V at most λ of the times.

By cyclically shifting each of the set S_i m -times (mod v), $b=tm$ different sets can be created. By considering the elements of b sets as positions of ones of corresponding columns in an element-block incidence matrix, it can be verified that such obtained incidence matrix

has the properties of a parity-check matrix H of corresponding LDPC code. By selecting the index $\lambda=1$, it can be verified that the matrix- H has the girth of at least 6.

Theorem 1. If $20t+1$ is a prime or a prime power, and θ is a primitive root of $\text{GF}(20t+1)$, the following t initial sets $S_0=(\theta^0, \theta^{4t}, \theta^{8t}, \theta^{12t}, \theta^{16t})$, $S_2=(\theta^2, \theta^{4t+2}, \theta^{8t+2}, \theta^{12t+2}, \theta^{16t+2})$, ..., $S_{2t}=(\theta^{2t-2}, \theta^{6t-2}, \theta^{10t-2}, \theta^{14t-2}, \theta^{18t-2})$ form a difference system with following parameters

$$v = 20t + 1, \quad k = 5, \quad \lambda = 1 \quad (10)$$

The number of blocks in this difference system is $b=t(20t+1)$. The corresponding LDPC code has the length $N=t(20t+1)$, the number of parity bits $N-K=20t+1$, the code rate is lower bounded by $R \geq 1-1/t$, and the girth is at least six.

This theorem can easily be proved in a fashion similar to the proof of Theorem 7.1.5 in [18]. For code rates above 0.9 the parameter t must be greater than or equal to 10. Notice that ITU-T G.975 standard for fiber optics communications limits the allowed forward error correction (FEC) overhead to 7%, so that design of LDPC codes with code rates above of 0.9 is extremely important. At the same time large decoding delay cannot be tolerated because of extremely high speeds, and LDPC codes of medium lengths are necessary. For example, by selecting $t=14$, an LDPC code of rate $R=1-1/14=0.93$ with 7.7% of overhead is obtained. The codeword length is $N=14(20 \cdot 14+1)=3934$, and the number of parity bits $N-K=20 \cdot 14+1=281$. An interesting property of parity-check matrix obtained using this design is that H -matrix is of a full-rank, so someone does not need to do Gaussian elimination to determine the code rate. Moreover, H -matrix can be written as

$$H = \begin{bmatrix} H_1 & H_2 & \dots & H_t \end{bmatrix}, \quad (11)$$

with sub-matrix H_i corresponding to set S_i and all its $(20t+1)$ -cyclic shifts. Each sub-matrix H_i can be split into 20 permutation matrices blocks plus single-parity check equation, suggesting that H -matrix (11) has highly regular structure, and the same structure may be re-used at different levels during implementation of an LDPC decoder. To create the generator matrix using (11), the full inversion is not required, we may proceed in a fashion similar to that we reported in [23]. To increase the girth of corresponding bipartite graph to 8, we propose to selectively remove the several sub-matrices in (11), using an algorithm similar to that we reported in [24]. The second class of LDPC codes is based on concept of *product of combinatorial designs*, such as balanced incomplete block designs (BIBDs), 1-configurations, orthogonal arrays (OAs), or Mutually orthogonal Latin rectangles [18,19].

Definition 2. A λ -configuration, denoted as t - $(v, k, \{0, 1, \dots, \lambda\})$, is a collection of k -subsets (*blocks*) of a v -set V such that every t -subset of V is contained in *at most* λ of the blocks.

Codes based on λ -configurations with $\lambda > 1$ and $t \geq 2$ have the girth 4, and therefore we will restrict our attention to the case $\lambda=1$ and $t=2$, because the corresponding bipartite graph has the girth at least 6. Notice that a BIBD is a special case of λ -configuration, in which $t=2$, and every 2-subset of V is contained in *exactly* λ of the blocks. Let us now introduce the concept of product of combinatorial designs, say λ -configurations. Notice that the concept of Kronecker-product designs has already be introduced by Vartak (1955) [22], however, such a definition leads to girth-4 LDPC codes, and as such is not of interest in this paper.

Definition 3. Let λ_1 - and λ_2 -configurations, denoted as t - $(v_1, k_1, \{0, 1, \dots, \lambda_1\})$ and t - $(v_2, k_2, \{0, 1, \dots, \lambda_2\})$, be given. Denote the number of blocks in λ_1 - and λ_2 -configurations by b_1 and b_2 , respectively; and the corresponding set of blocks by B_1 and B_2 , respectively. The $v_1 v_2$ -elements in the product configuration are ordered pair of elements (e_1, e_2) , with e_1 belonging to B_1 and e_2 belonging to B_2 . $b = \lfloor b_1/k_1 \rfloor \lfloor b_2/k_2 \rfloor$ blocks of a product configuration are obtained as follows (with $\lfloor \cdot \rfloor$ we denoted the largest integer less than or equal to the enclosed quantity). Let the blocks from B_1 be grouped into $\lfloor b_1/k_1 \rfloor$ classes of k_1 blocks each. The first block in a product configuration is obtained as a $k_1 k_2$ -block of ordered pair of elements $((\alpha_1, \beta_1), \dots, (\alpha_1, \beta_{k_2}), \dots, (\alpha_{k_1}, \beta_1), \dots, (\alpha_{k_1}, \beta_{k_2}))$, with α_i ($i=1, \dots, k_1$) belonging to the first block of B_1 , and β_i ($i=1, \dots, k_2$) belonging to the first block in B_2 . The first class in product design is obtained by

taking one block from the first class in B_1 at the time, and one block in B_2 out of the first k_2 blocks, and create a product block as explained above. The second class in product design is obtained by observing next k_1 blocks in B_1 , and next k_2 blocks in B_2 . The procedure is repeated until all blocks in either B_1 or B_2 are exploited, or b blocks are generated. The blocks already used in creating the previous product blocks are excluded from further consideration. The product of P configurations can be defined iteratively by taking the product of two configurations in each step.

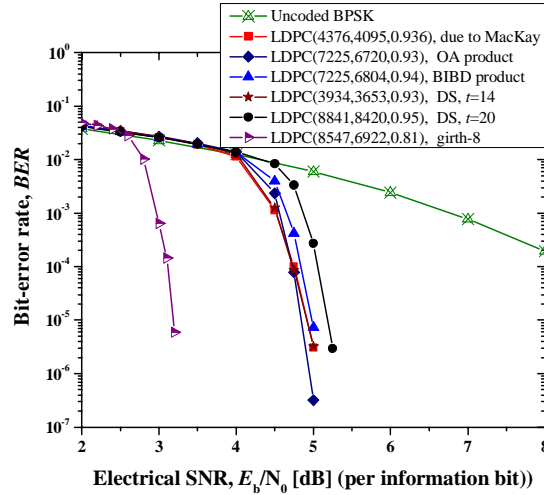


Fig. 3. BER performance of proposed LDPC codes on an AWGN channel

Example. Let us observe the product of a $(6,2,\{0,1\})$ configuration composed of set of blocks $B_1 = \{\{1,4\}, \{2,5\}, \{3,6\}, \{1,5\}, \{2,6\}, \{3,4\}, \{1,6\}, \{2,4\}, \{3,5\}\}$ with itself. The resulting product configuration has $v_1 v_2 = v^2 = 36$ elements $(1,1), \dots, (1,6), \dots, (6,1), \dots, (6,6)$; there are $b = \lfloor b/k \rfloor^2 = 16$ blocks, and each of the block is of size $k^2 = 4$. By listing the two-dimensional elements $(1,1), \dots, (6,6)$ as integers $1, 2, \dots, 36$ the resulting product configuration $(36,4,\{0,1\})$ has the following blocks:

$B = \{\{1,4,19,22\}, \{2,5,20,23\}, \{7,10,25,28\}, \{8,11,26,29\}, \{15,18,33,36\}, \{13,17,31,35\}, \{3,6,27,30\}, \{1,5,25,29\}, \{8,12,32,36\}, \{9,10,33,34\}, \{14,18,20,24\}, \{15,16,21,22\}, \{1,6,31,36\}, \{2,4,32,34\}, \{7,12,19,24\}, \{8,10,20,22\}\}$.

Theorem 2. Let us observe the product of P 1-configurations denoted by $2-(v_i, k_i, \{0,1\})$ ($i=1, \dots, P$). By identifying the integers in every block of a product configuration obtained as explained in Definition 3 as positions of ones in corresponding rows in a block-element incident matrix, we can establish 1-to-1 correspondence between a block-element incident matrix and a parity-check matrix of an equivalent LDPC code. An LDPC code such obtained has the girth of at least 6, the codeword length is $v_1 v_2 \dots v_p$, and the code rate is lower bounded by

$$R \geq 1 - \lfloor b_1/k_1 \rfloor \dots \lfloor b_p/k_p \rfloor / (v_1 v_2 \dots v_p). \quad (12)$$

Using the concepts we introduced in Ref. [24], and Definition 3 it is straightforward to prove the Theorem 2. In example above the codeword length is $v_1 v_2 = 36$, the number of parity bits $b = \lfloor b_1/k_1 \rfloor \cdot \lfloor b_2/k_2 \rfloor = 16$, and the girth of corresponding bipartite graph is 8. It can also be shown that in most of the cases the in-equality (12) is satisfied with equality, meaning that the parity-check matrix of an LDPC code designed using Definition 3, and Theorem 2 has a full-rank.

The results of simulations for two classes of LDPC codes introduced in this section are shown in Fig. 3, for an AWGN channel model. The girth-6 code of rate 0.95 and length 8841 is designed using Theorem 1 for $t=21$, while the girth-6 code of rate 0.93 and length 3934 is designed for $t=14$. The girth-8 (8547, 6922) LDPC code of rate 0.81 is designed starting from

girth-6 by selectively removing the sub-matrices in (11). The LDPC codes (7225, 6720) and (7225, 6804) are obtained using Theorem 2 for two initial 1-configurations obtained based on OAs and BIBDs, respectively. The bit-error rate (BER) performance of proposed LDPC codes are comparable to or better than random (4376, 4095) LDPC code due to MacKay [25].

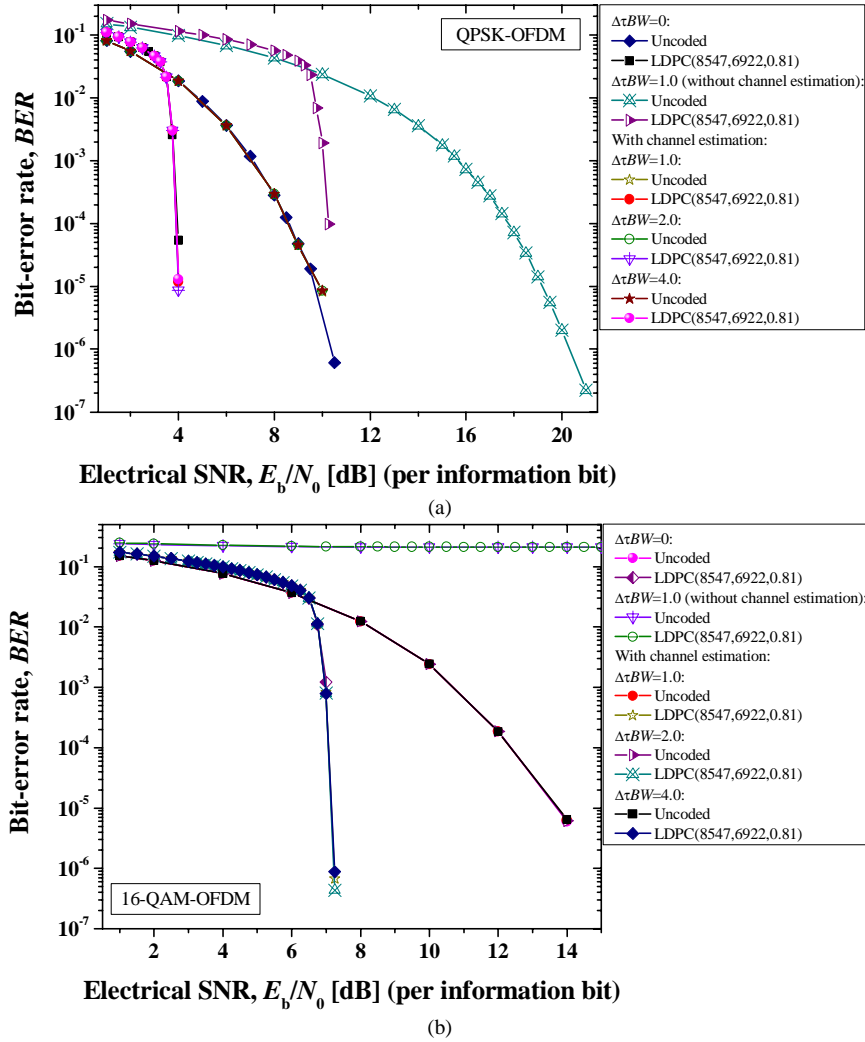


Fig. 4. BER performance of LDPC(8547,6922)-coded OFDM for different DGD values, and: (a) QPSK, or (b) 16-QAM. The power-splitting ratio between two PSPs was set to $k=1/2$.

4. Numerical results

The results of simulations, for U-OFDM and thermal noise dominated scenario, are shown in Figs. 4-5 for different DGDs, and the worst-case scenario ($k=1/2$). The OFDM signal bandwidth is set to $BW=0.25B$ (B -is the aggregate bit rate set to 10Gb/s), the number of sub-channels is set to $N_{QAM}=64$, FFT/IFFT is calculated in $N_{FFT}=128$ points, RF carrier frequency is set to $0.75B$, the bandwidth of optical filter for SSB transmission is set to $2B$, and the total averaged launched power is set to 0 dBm. The guard interval is obtained by cyclic extension of $N_G=2 \times 16$ samples. The Blackman-Harris windowing function is applied, and OFDM symbol period is $0.06544 \mu s$. QPSK-OFDM and 16-QAM-OFDM with and without channel estimation are observed in simulations. The effect of PMD is reduced by: (i) using sufficient

number of sub-carriers so that the OFDM symbol rate is significantly lower than aggregate bit rate, and (ii) using the short training sequence (of duration of one OFDM symbol) to estimate the PDM distortion. To improve the BER performance further two classes of LDPC codes introduced in previous Section are employed in simulations.

For DGD of $1/BW$ RZ-OOK threshold receiver is not able to operate properly at all because it enters BER error floor. QPSK-OFDM receiver itself, however, is able to operate error free as shown in Fig. 4. The simple channel estimation technique proposed in Section 3 provides significant reduction of distortion due to PMD. The improvement due to channel estimation is about 10dB at BER of 10^{-6} . LDPC code of rate 0.81 provides additional 6dB improvement at the same BER. Notice that 16-QAM-OFDM without channel estimation enters BER floor, and even advanced FEC cannot help too much in reducing the BER. A girth-6 LDPC code of rate 0.93 (with 7.7% of overhead) performs about 2dB worse than girth-8 LDPC code of rate 0.81 (with 25% of overhead). LDPC-coded QPSK-OFDM scheme outperforms LDPC-coded 16-QAM-OFDM scheme by about 3dB at BER of 10^{-6} .

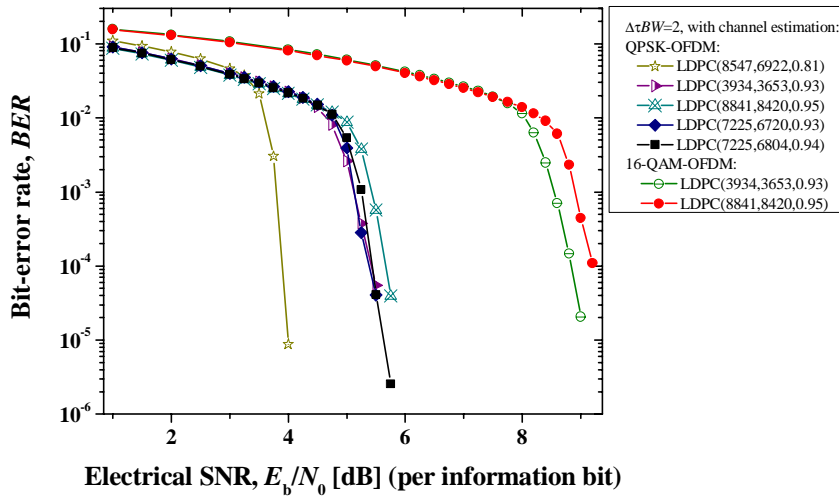


Fig. 5. BER performance of LDPC-coded OFDM for different DGD values, and different LDPC codes of rate $R \geq 0.93$. The power-splitting ratio between two PSPs was set to $k=1/2$.

5. Conclusion

We discussed the possibility of PDM compensation in fiber-optics communication systems using appropriate channel estimation and LDPC-coded OFDM with direct detection. Two classes of high-rate LDPC codes, based on difference systems and a product of combinatorial designs are introduced. A simple channel estimation technique is able to compensate first-order PMD for DGD of $4/BW$ in LDPC-coded OFDM systems. The proposed PMD-compensation scheme is an excellent PMD-compensator candidate, capable of compensating DGDs above two bit-periods. For DGDs below two bit periods LDPC-coded turbo equalization can also be used in PMD-compensation. Important advantages of OFDM with direct detection over coherent OFDM are: (i) insensitivity to the laser phase noise, (ii) lower complexity receiver implementation, and (iii) compatibility with already installed IM/DD systems.